

Structural, electronic, and optical properties of wurtzite and rocksalt InN under pressure

Man-Yi Duan,^{1,2} Lin He,¹ Ming Xu,^{1,3,*} Ming-Yao Xu,² Shuyan Xu,⁴ and Kostya (Ken) Ostrikov^{5,6}

¹*Institute of Solid State Physics, Sichuan Normal University, Chengdu 610068, People's Republic of China*

²*School of Science, Wuhan University of Science and Engineering, Wuhan 430073, People's Republic of China*

³*International Center for Material Physics, CAS, Shenyang 110016, People's Republic of China*

⁴*Natural Sciences, National Institute of Education, NTU, 637616 Singapore, Singapore*

⁵*CSIRO Materials Science and Engineering, P.O. Box 218, Lindfield, New South Wales 2070, Australia*

⁶*School of Physics, The University of Sydney, Sydney, New South Wales 2006, Australia*

(Received 21 May 2009; revised manuscript received 17 August 2009; published 13 January 2010)

Structural stability, electronic, and optical properties of InN under high pressure are studied using the first-principles calculations. The lattice constants and electronic band structure are found consistent with the available experimental and theoretical values. The pressure of the wurtzite-to-rocksalt structural transition is 13.4 GPa, which is in an excellent agreement with the most recent experimental values. The optical characteristics reproduce the experimental data thus justifying the feasibility of our theoretical predictions of the optical properties of InN at high pressures.

DOI: [10.1103/PhysRevB.81.033102](https://doi.org/10.1103/PhysRevB.81.033102)

PACS number(s): 71.15.Mb, 71.55.Eq, 74.25.Gz

Indium nitride (InN) is a promising material for technological developments because of a very narrow direct band gap, superior carrier transport characteristics and electrical conductivity in a wide range of temperatures.¹ Under high pressures, InN experiences phase transitions from the wurtzite-to-the-rocksalt structure.² However, there are significant discrepancies between the transition pressures reported in theoretical^{3–5} and experimental studies.^{6–10} Moreover, since the properties of InN are sensitive to external pressure, exploring the electronic and optical properties of InN under high pressures is important.

Here, we study the structural, electronic and optical properties of wurtzite and rocksalt InN under high pressure. The results are in a good agreement with the recent experimental and theoretical data. We also predict the optical characteristics of InN at high pressures.

We have used the first-principles pseudopotential plane-wave method based on the density-functional theory (DFT) incorporated into the CASTEP computational code. Ultrasoft pseudopotential with $4d^{10}5s^25p^1$ and $2s^22p^3$ valence-electron configurations for In and N atoms, respectively, were used. The exchange and correlation potentials are described in the framework of the generalized gradient approximation (GGA) and the local-density approximation (LDA). In the wurtzite InN, the In and N atom positions are In(0,0,0), In(1/3,2/3,1/2), N(0,0, u), and N(1/3,2/3, $u+1/2$), where u is a dimensionless parameter that represents the distance between the In plane and its nearest-neighbor N plane, expressed in the units of the lattice parameter c . On the other hand, the In and N atom positions in the rocksalt InN structure are In(0,0,0), and N(1/2,1/2,1/2), respectively. The plane-wave cutoff energy was assumed to be 750 eV, while the Brillouin-zone sampling mesh parameters for the k-point set were chosen as $12 \times 12 \times 6$ and $12 \times 12 \times 12$ for the wurtzite and the rocksalt phases of InN, respectively. The maximum magnitudes of the force on the atom, stress, and atomic position displacement between computational cycles were maintained below 0.01 eV/Å, 0.02 GPa, and 5×10^{-4} Å, respectively.

To confirm the transition pressure between the wurtzite and rocksalt structural phases of InN, we have calculated the

Gibbs free energy $H=E+PV+TS$ for the two phases. The $E-V$ and $G-P$ curves are shown in Fig. 1. The transition pressure P_t deduced from either the $E-V$ or $G-P$ curves are

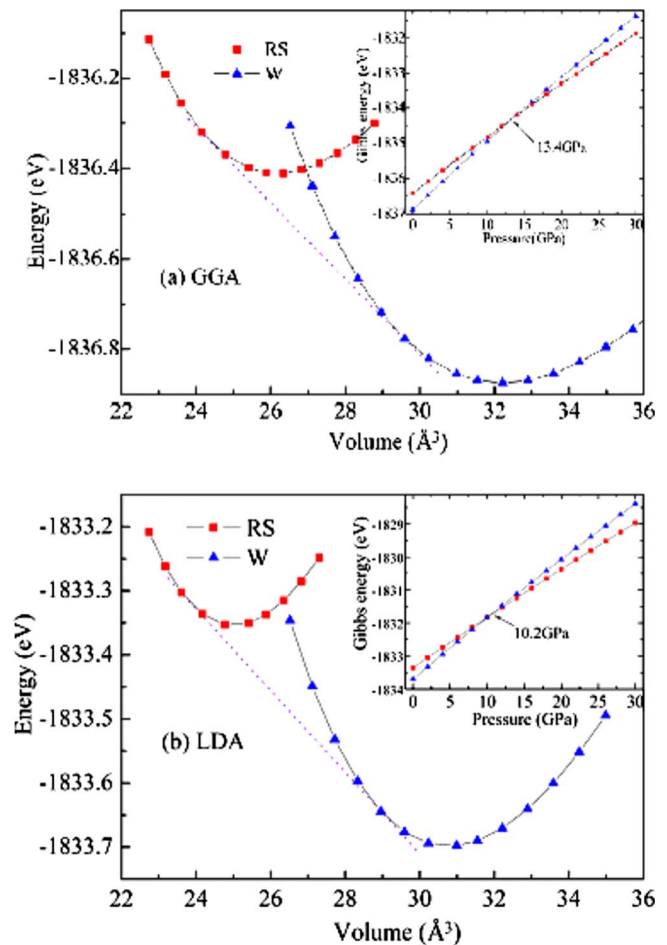


FIG. 1. (Color online) The energy as a function of volume, the inset is the Gibbs energy as a function of pressure for both wurtzite and rocksalt structural phases of InN calculated in the framework of (a) GGA and (b) LDA.

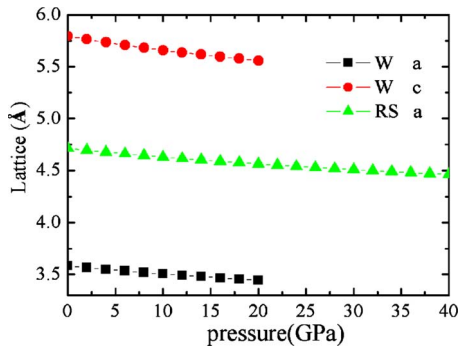


FIG. 2. (Color online) The variation in the lattice constants versus pressure for wurtzite and rocksalt InN.

approximately 13.4 GPa for GGA and 10.2 GPa for LDA cases. Our result obtained using the GGA is in an excellent agreement with the most recent experimental value 13.5 ± 0.5 GPa measured by Raman scattering.⁹ Compared to the LDA-predicted values calculated in this work [10.2 GPa, shown in Fig. 1(b)] and by other authors (10.86 GPa³ and 11.1 GPa⁵), indicating that the calculations based on the GGA are much more accurate to predict the phase-transition pressure.^{3,11} This fact will also support the validity of our theoretical predictions of other properties of InN under high-pressure conditions.

The computed values of the lattice constants as a function of pressure are plotted in Fig. 2; all the lattice constants decrease as the pressure increases. The equilibrium lattice constants a_0 of wurtzite and rocksalt structure are 3.583 and 4.712 Å at normal (zero external) pressure, respectively, in accordance with the values calculated by other authors.^{3,12,13} The calculated lattice constants of wurtzite InN at zero external pressure are in an excellent agreement with the experimental results.⁷ Even at 20 GPa, the calculated value (4.562 Å) of rocksalt InN still exhibits a very good agreement with the experimental value 4.535 ± 0.001 Å obtained by x-ray diffractometry.⁶ Figure 3 shows the dependence of the relative volume of the wurtzite and the rocksalt InN phases on the external pressure. The relative volume decreases almost linearly with the pressure, reasonably close to the experimental data.^{6,7}

Figure 4(a) shows the band structure of the wurtzite InN

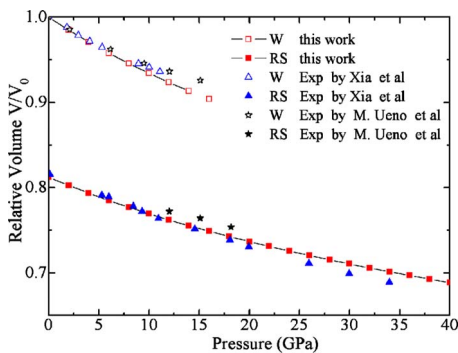


FIG. 3. (Color online) Changes of the relative volume of wurtzite and rocksalt InN with increasing pressure. The squares are this work; the triangles and stars from Refs. 6 and 7, respectively.

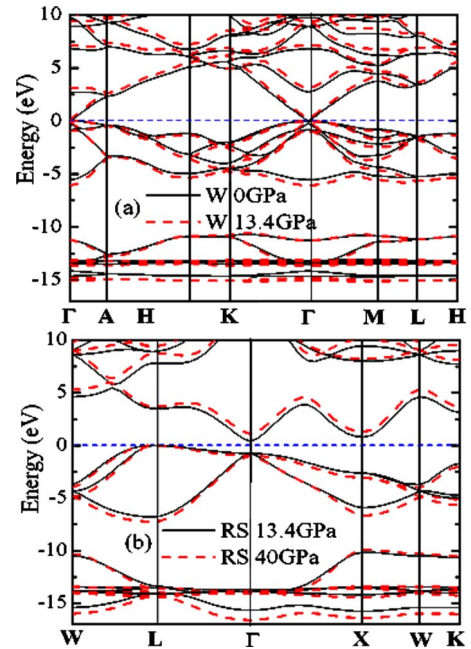


FIG. 4. (Color online) Band structure: (a) wurtzite InN under 0 and 13.4 GPa (b) rocksalt InN under 13.4 and 40 GPa.

phase with and without the external pressure of 13.4 GPa. Under no-external-pressure conditions, an almost zero direct band gap can be observed at a highly symmetric Γ point, close to the theoretical value,¹⁴ yet smaller than the experimental value reported.¹⁵ This underestimate, which is very common to most of the DFT approximations,^{11,16} can be reduced by using the energy scissor approximation.^{17,18}

From the band structure of the rocksalt InN under 13.4 and 40 GPa shown in Fig. 4(b), one can note that the conduction-band minimum is located at the Γ point, while the valence-band maximum is located at the L point, indicating that the rocksalt InN is an indirect band-gap semiconductor. The topmost electron levels of the valence band are threefold degenerate at the Γ point, and twofold degenerate at the L and X points. When the pressure increases, the valence band tends to broaden and shift toward the lower-energy region whereas the conduction-band levels shift toward the higher-energy region for both low- and high-pressure structural phases. Indeed, interatomic spacing is expected to decrease as the pressure becomes higher. Under such conditions, the wave functions overlap more strongly. Thus, there is an increase in the dispersion of the bands in k space as well as in the bandwidths. Hence, the band gap broadens at higher pressures.

In Fig. 5, the distribution of the density of states of the wurtzite and the rocksalt InN over the energy spectrum is presented. The valence band can be divided into two zones. The lower part of the valence band (from -16.5 to approximately -10.0 eV) is mostly composed of In $4d$ and N $2s$ states, where the In $4d$ states exhibit quite strong localization. On the other hand, the upper part of the valence band (from -7.5 to 0.0 eV) contains N $2p$ states coupled with In $5p$ and In $5s$ states. The most prominent unoccupied energy bands in the lowest energy domain of the conduction

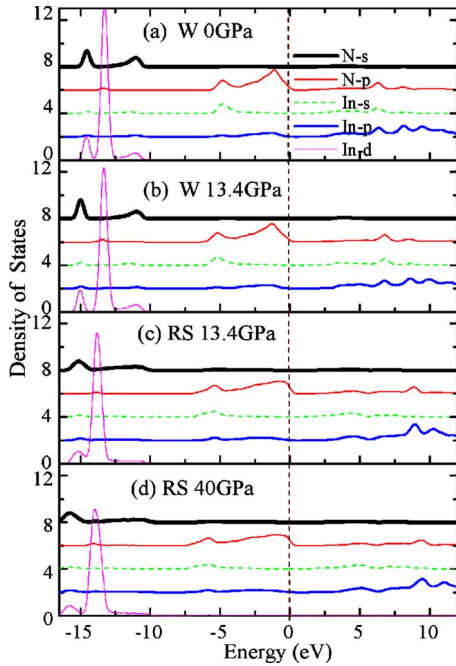


FIG. 5. (Color online) Density of states for N $2s$, N $2p$, In $5s$, In $5p$, and In $4d$. (a) wurtzite InN under no-external-pressure conditions; (b) wurtzite InN under 13.4 GPa (c) rocksalt InN under 13.4 GPa, and (d) rocksalt InN under 40 GPa.

band are composed of s and p states from In and p states from N, notably without any d states. The p states of In seem to be dominant. Moreover, the intensity of In $4d$ states in the valence bands of InN clearly decreases as the pressure increases.

Figure 6(a) shows the imaginary part $\varepsilon_2(\omega)$ of the complex dielectric function $\varepsilon(\omega) = \varepsilon_1(\omega) + i\varepsilon_2(\omega)$, where the open circles represent the experimental data. Without the external pressure, there is an excellent agreement with the experimentally measured optical responses and other numerical results.^{2,19,21} There are two main peaks at 5.3 and 10.0 eV in the $\varepsilon_2(\omega)$ spectrum of the wurtzite InN under no-pressure conditions. The peak at 5.3 eV takes its origin from the optical transitions between N $2p$ states in the valence band and In $5p$ states in the conduction band, while the other peak at 10.0 eV is caused by the optical transitions from $5p$ and $5s$ states of In to N $2p$ states. When the pressure increases from 0 to 13.4 GPa, the spectrum exhibits a small blueshift (~ 0.5 eV) without any notable shape changes. This is an interesting and quite unusual feature since the electronic bands maintain the shape/structure when the band gap is broadened.

The calculated $\varepsilon_1(\omega)$ [Fig. 6(b)] also shows a good agreement with the experimental values²¹ and other calculations^{19,22} for the wurtzite InN without any external pressure. The $\varepsilon_1(\omega)$ spectra exhibit a rather steep decrease in the range between 5 and 7 eV. Above this range, $\varepsilon_1(\omega)$ of the rocksalt phase InN becomes negative, and further reaches a minimum followed by a slow increase to zero. Another minimum of $\varepsilon_1(\omega)$ is at around 12 eV, and $\varepsilon_1(\omega)$ increases up to the zero level at higher energies. For wurtzite phase InN,

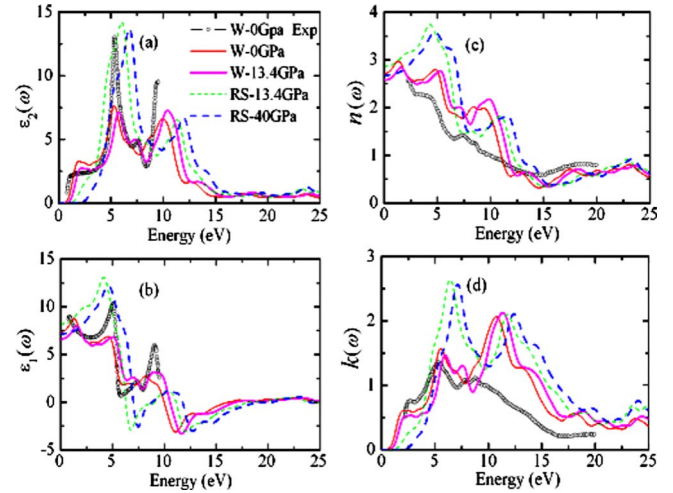


FIG. 6. (Color online) (a) Imaginary part of dielectric function $\varepsilon_2(\omega)$; (b) real part of dielectric function $\varepsilon_1(\omega)$; (c) refractive index $n(\omega)$; and (d) extinction coefficient $k(\omega)$ of wurtzite InN under 0 and 13.4 GPa and rocksalt InN under 13.4 and 40 GPa. The experimental data (a) and (b) from Ref. 21, (c) and (d) from Ref. 23.

$\varepsilon_1(\omega)$ spectrum exhibits only one negative region in the range of 10–12 eV.

The refractive index $n(\omega)$ and the extinction coefficient $k(\omega)$ have also been calculated for wurtzite InN under 0 and 13.4 GPa and the rocksalt InN under 13.4 and 40 GPa external pressures, as displayed in Figs. 6(c) and 6(d), respectively. For wurtzite InN under no-external-pressure conditions, the static refractive index is $n_0 = 2.7$. Moreover, n_0 of both wurtzite and rocksalt InN decreases as the pressure increases. The $k(\omega)$ shows two main peaks at around (5.9 and 11.2 eV) and (6.4 and 11.7 eV) for the wurtzite and the rocksalt InN at 13.4 GPa, respectively. For the wurtzite InN, the peak intensity at around 6.4 eV is stronger than that at ~ 5.9 eV. Both the refractive index and the extinction coefficient shift toward the higher-energy region when the pressure increases.

We stress that at high pressures the refractive index of InN in the 2.8–7.3 eV range is up to 2 times higher than under normal conditions. The extinction coefficient, in turn, decreases in the 2.6–5.1 eV range and increases in the 5.1–7.5 eV range. One can thus expect much stronger refraction and much weaker damping of the light with photon energies between 2.8 and 5.1 eV.

In conclusion, we studied the structural stability, electronic band structure, electronic density of states, and optical properties of wurtzite and rocksalt InN under pressure. The calculated lattice constant and the transition pressure are in a very good agreement with the experimental results. The wurtzite InN is a direct band-gap semiconductor, while the rocksalt InN is an indirect band-gap semiconductor. As the pressure increases, the valence-band levels shift toward the lower-energy domain whereas the conduction-band levels shift toward the higher-energy region. This allowed us to predict the variation of the optical properties for the rocksalt or wurtzite InN under pressure.

*Corresponding author; hsuming_2001@yahoo.com.cn

- ¹T. L. Tansley and C. P. Foley, *J. Appl. Phys.* **59**, 3241 (1986).
- ²N. E. Christensen and I. Gorczyca, *Phys. Rev. B* **50**, 4397 (1994).
- ³S. Saib and N. Bouarissa, *Physica B* **387**, 377 (2007).
- ⁴A. M. Saitta and F. Decremps, *Phys. Rev. B* **70**, 035214 (2004).
- ⁵C. C. Silva, H. W. Leite Alves, L. M. R. Solfaro, and J. R. Leite, *Phys. Status Solidi C* **2**, 2468 (2005).
- ⁶Q. Xia, H. Xia, and A. L. Luoff, *Mod. Phys. Lett. B* **8**, 345 (1994).
- ⁷M. Ueno, M. Yoshida, A. Onodera, O. Shimomura, and K. Takemura, *Phys. Rev. B* **49**, 14 (1994).
- ⁸C. Pinquier, F. Demangeot, and J. Frandon, *Phys. Rev. B* **70**, 113202 (2004).
- ⁹C. Pinquier, F. Demangeot, J. Frandon, J. C. Chervin, A. Polian, B. Couzinet, P. Munsch, O. Briot, S. Ruffenach, B. Gil, and B. Maleyre, *Phys. Rev. B* **73**, 115211 (2006).
- ¹⁰A. Munoz and K. Kunc, *J. Phys.: Condens. Matter* **5**, 6015 (1993).
- ¹¹A. J. Cohen, P. Mori-Sanchez, and W. Yang, *Science* **321**, 792 (2008).
- ¹²J. Serrano, A. Rubio, E. Hernández, A. Muñoz, and A. Mujica, *Phys. Rev. B* **62**, 16612 (2000).
- ¹³C. Stampfl and C. G. van de Walle, *Phys. Rev. B* **59**, 5521 (1999).
- ¹⁴A. Janotti, D. Segev, and C. G. van de Walle, *Phys. Rev. B* **74**, 045202 (2006).
- ¹⁵T. Matsuoka, H. Okamoto, M. Nakao, H. Harima, and E. Kurimoto, *Appl. Phys. Lett.* **81**, 1246 (2002).
- ¹⁶L. J. Sham and M. Schlüter, *Phys. Rev. Lett.* **51**, 1888 (1983).
- ¹⁷Underestimates of the optical band-gap values are common to either LDA or GGA. The scissor operation is reasonably accurate for the prediction of the optical properties of InN. More advanced methods such as GW quasiparticle method (Ref. [19](#)) or DFT+*U* (Ref. [20](#)) could possibly improve the accuracy.
- ¹⁸H. M. Weng, X. P. Yang, J. M. Dong, H. Mizuseki, M. Kawasaki, and Y. Kawazoe, *Phys. Rev. B* **69**, 125219 (2004).
- ¹⁹J. Furthmüller, P. H. Hahn, F. Fuchs, and F. Bechstedt, *Phys. Rev. B* **72**, 205106 (2005).
- ²⁰A. Walsh, J. L. F. Da Silva, and S. H. Wei, *Phys. Rev. Lett.* **100**, 256401 (2008).
- ²¹R. Goldhahn, A. T. Winzer, V. Cimalla, O. Ambacher, C. Cobet, W. Richter, N. Esser, J. Furthmüller, F. Bechstedt, H. Lu, and W. J. Schaff, *Superlattices Microstruct.* **36**, 591 (2004).
- ²²Y. N. Xu and W. Y. Ching, *Phys. Rev. B* **48**, 4335 (1993).
- ²³Q. Guo, O. Kato, M. Fujisawa, and A. Yoshida, *Solid State Commun.* **83**, 721 (1992).